sible, for example, if the carriers come from two distinct portions of the Fermi surface. Bennett[2] has studied the region of the Fermi surface of lead which contributes to the tunneling current in the [110], [111], and [100] directions (Fig. 9). Using this information and the Anderson and Gold four-parameter model for the Fermi surface of lead, the Fermi velocities of the different components in the tunneling current were computed. The results do not agree at all well with the measured values. In particular, one component has a velocity about twice the value of any of the computed ones. This discrepancy remains unexplained and is worthy of further study.

*Work supported by the U. S. Air Force Office of Scientific Research under Grant No. AF-AFOSR-1241-7 and by the Advanced Research Projects Agency of the Department of Defense to the University of North Carolina, Chapel Hill, N. C. 27514.

†Present Address: Physics Department, University of North Dakota, Grand Forks, N. D.

‡Present Address: Physics Department, University of Idaho, Moscow, Ida. 83843.

[1]N. V. Zavaritskii, Zh. Eksperim. i Teor. Fiz. 45, 1839 (1963) [Sov. Phys. JETP 18, 1260 (1964)].

[2]A. J. Bennett, Phys. Rev. 140, A1902 (1965).

[3]B. L. Blackford and R. H. March, Phys. Rev. 186, 397 (1969).

[4]G. L. Wells, J. E. Jackson, and E. N. Mitchell, Phys. Rev. B 1, 3636 (1970).

[5]R. C. Dynes and J. P. Carbotte, Physica (to be published).

[6]W. J. Tomasch, Phys. Rev. Letters 15, 672 (1965).

[7]W. L. McMillan and P. W. Anderson, Phys. Rev. Letters 16, 85 (1966).

[8]G. I. Lykken, A. L. Geiger, and E. N. Mitchell, Phys. Rev. Letters 25, 1578 (1970).

[9]T. Schober, J. Appl. Phys. 40, 4658 (1969).

[10]J. D. Landry and E. N. Mitchell, J. Appl. Phys. 40, 3400 (1969).

[11]J. G. Adler and J. E. Jackson, Rev. Sci. Instr. 30, 1049 (1966).

[12]M. L. A. McVicar and R. M. Rose, J. Appl. Phys. 39, 1721 (1968).

[13]B. L. Blackford, Physica (to be published).

[14]T. Wolfram, Phys. Rev. 170, 481 (1968).

[15]W. L. McMillan, Phys. Rev. 175, 559 (1968).

[16]W. J. Tomasch, in *Tunneling Phenomena in Solids*, edited by E. Burstein and S. Lundquist (Plenum, New York, 1969).

[17]W. L. McMillan and J. M. Rowell, in *Superconductivity*, edited by R. D. Parks (Marcel Dekker, New York, 1969).

[18]K. Maki and A. Griffin, Phys. Rev. 150, 356 (1966).

[19]J. R. Anderson and A. V. Gold, Phys. Rev. 139, A1459 (1965).

[20]J. M. Rowell and W. L. McMillan, Physica (to be published).

PHYSICAL REVIEW B VOLUME 4, NUMBER 5 1 SEPTEMBER 1971

Quantized Flux States of Superconducting Cylinders*

William L. Goodman, Wayne D. Willis, Daniel A. Vincent, and Bascom S. Deaver, Jr.

Department of Physics, University of Virginia, Charlottesville, Virginia 22901

(Received 30 April 1971)

We have measured the magnetic flux trapped in hollow superconducting cylinders (14–56-μ i.d., 0.1–5-μ walls, 0.5–2.5 cm long) as a function of the applied magnetic field in which the cylinder was cooled through its transition temperature. For most applied fields, the entire cylinder is in the same quantum state; for some fields there is a mixed state with bands along the cylinder in states differing by one flux quantum. In cylinders with walls thick with respect to the penetration depth, the trapped flux is an integral multiple of $hc/2e \pm \frac{1}{2}\%$. We have measured the temperature dependence of the trapped flux in a cylinder containing a single flux quantum and find a continuous reversible change by just the amount required to maintain the constancy of the fluxoid.

I. INTRODUCTION

London introduced the concept of the fluxoid Φ defined for any closed path within a superconductor by

$$\Phi = \oint (4\pi\lambda^2/c)\vec{j}\cdot d\vec{s} + \oint \vec{A}\cdot d\vec{s} = n\Phi_0 \quad , \qquad (1)$$

where λ is the penetration depth, $\vec{j}$ the supercurrent density, and $\vec{A}$ the magnetic vector potential, and he predicted that Φ would be quantized.[1,2] This property of superconductors follows immediately from requiring that the macroscopic wave function be single valued. The quantum Φ_0 determined experimentally and related to the pairing of electrons by the microscopic theory is

$$\Phi_0 = hc/2e = 2.07\times10^{-7}\ \mathrm{G\,cm^2}. \qquad (2)$$

For a hollow superconducting cylinder with wall thickness large compared to the penetration depth, a path can be chosen along which the current is ar-

bitrarily small, and thus the first integral in Eq. (1) can be neglected. Then the total magnetic flux trapped by a persistent current in the cylinder is precisely quantized in units of Φ_0. The first experimental demonstrations of fluxoid quantization were obtained by measurements of quantized flux trapped in superconducting cylinders.[3-5] Immediately after these experiments there were a number of theoretical papers dealing with fluxoid quantization using both microscopic theories and various phenomenological theories.[6-25] All relate the factor of 2 in the quantum to the pairing of electrons in superconductors. Various properties of superconducting cylinders are discussed including the periodic variation of the free energy with flux in the cylinder, the stability of persistent currents, and the interpretation of the state of the cylinder as a macroscopic quantum effect.

Little and Parks[26] measured the periodic variation of the resistance of small superconducting cylinders (~1-μ diam) with enclosed magnetic flux and thus exhibited vividly a consequence of the periodic variation of the free energy by way of its effect on the transition temperature T_c and hence on the resistance near T_c. Kwiram and Deaver[27] observed the flux change as a superconducting cylinder was cyclically varied through T_c in an applied magnetic field and obtained magnetization curves which were periodic with enclosed flux with period Φ_0.

Using an electron interferometer, Lischke[28,29] and Boersch and Lischke[30] have observed the flux trapped in very small cylinders (0.3–0.5-μ i.d.) and find it is $n\Phi_0 \pm 4\%$. They observe that when several quanta are trapped in a tapered cylinder, the flux escapes in discrete steps of Φ_0 along the length.

For a cylinder with walls thin with respect to λ there is current even at the outer surface and thus the first integral in Eq. (1) cannot be neglected. In this case the trapped flux can be less than the full value $n\Phi_0$ and was first shown by Bardeen[9] to be

$$\varphi = n\Phi_0(1 + 2\lambda^2/rw)^{-1} \tag{3}$$

for a cylinder with radius r and wall thickness w. For a cylinder with walls so thin that the current density is uniform this result follows from Eq. (1) if the current and flux are related by $\varphi = iL$, where L is the inductance of a current sheet with the mean radius of the cylinder.[31] This result and expressions for the flux trapped in cylinders with walls of arbitrary thickness (which reduce to this result for very thin walls) have been obtained from microscopic theory, Ginsburg-Landau theory, and from various other models.[8,10,16,18,19,24,25] From Eq. (3) it is evident that even at very low temperature, for sufficiently small thin-walled cylinders, the trapped flux will differ from $n\Phi_0$; for any cylinder near T_c, as λ becomes large, the flux φ should be less than $n\Phi_0$.

Mercereau and Crane[32] and Hunt and Mercereau[33] have verified the constancy of the fluxoid by observing the reversible variation of the flux with temperature in rings containing 10^5–10^7 flux quanta. They find agreement with the temperature variation expressed through $\lambda(T)$ in Eq. (3). Using an electron interferometer to observe the flux in very small cylinders containing one of a few quanta, Lischke[34] finds no reduction due to very thin walls and no variation from $n\Phi_0$ with temperature.

Recently Goodman and Deaver[35] reported experiments using a superconducting magnetometer to measure the flux trapped in small cylinders. For most values of the initial applied magnetic field the entire cylinder was found to be in the same quantum state with $\Phi = n\Phi_0 \pm 1\%$. For some initial applied fields the cylinder was found to exhibit a mixed state with bands along the length of the cylinder in states differing by one flux quantum. Pierce[36] has proposed a model consisting of domains with alternating circulation along the length of the cylinder to account for these observations. He shows that the domains are metastable once they are established and discusses mechanisms for nucleating them.

We report here refinements of the measurements of Goodman and Deaver along with new results on the temperature dependence of the trapped flux. The domain structure has been observed with much better resolution; the total magnetic moment of the cylinder is shown to vary almost continuously with applied field, thus accounting in detail for the apparent contradiction of precise quantization posed by observed trapped flux values other than $n\Phi_0$ when the average flux in the whole cylinder is measured. Also the flux is measured as a function of temperature when the entire cylinder is in the same quantum state and reversible variations in good agreement with Eq. (3) are found.

II. TOTAL FLUX MEASUREMENTS

In the original experiments of Deaver and Fairbank[3] and of Doll and Näbauer.[4,5] the average flux trapped in small superconducting cylinders or the total magnetic moment of the cylinders was measured. Our initial experiments essentially repeated these measurements with a magnetometer of very much higher sensitivity. Most of the superconducting cylinders were formed by evaporating Sn or In onto a copper wire insulated with Formvar. The end of the wire was connected to a copper block cooled with liquid nitrogen during the evaporation to obtain more uniform films than resulted when the substrate was not cooled. Cylinders 14–56-μ i.d., with walls 1000–5000 Å thick and 0.5–2.5 cm long, were used. A few cylinders with walls up to 5 μ thick were made by electroplating Sn directly onto copper wires.

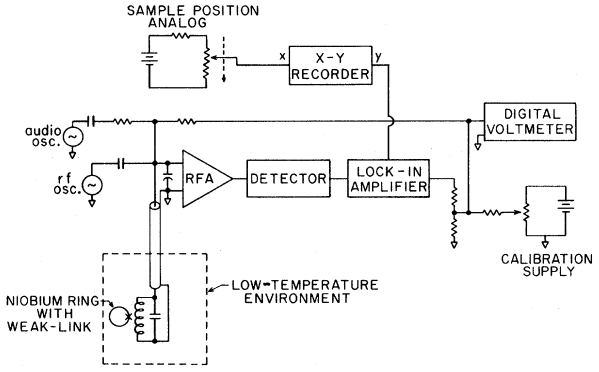

FIG. 1. Diagram of electronics used for operating superconducting magnetometers.

Measurements were made with a superconducting magnetometer similar in concept to the one described by Silver and Zimmerman.[37] A niobium ring with an adjustable point contact was coupled to the inductor of a tank circuit tuned to about 30 MHz and driven with a constant-current source (see Fig. 1). A small audio-frequency magnetic field was applied to the Nb ring producing a modulation of the rf which was phase sensitive to the flux linking the ring. The audio signal was fed to a lock-in amplifier whose output was fed back to a long solenoid inside the Nb ring. When the feedback loop was closed, the flux within the ring was constrained to remain constant, and the current flowing in the solenoid became a direct measure of flux changes through the ring.

The configuration used for total flux measurements is shown in Fig. 2. The solenoid marked "calibration coil" was used for the feedback current from the lock-in amplifier. The aluminum cylinder surrounding the sample was many skin depths thick to shield the sample from rf fields.

A few centimeters above the magnetometer and coaxial with it was mounted a long solenoid within which a known field could be applied to the sample cylinder. The sample cylinder was enclosed in a small glass or quartz tube mounted at the tip of an aluminum rod used to move the sample from the solenoid into the magnetometer. One end of the copper wire on which the sample cylinder was deposited was connected to a carbon resistor mounted in a cavity inside the aluminum rod. This resistor was used to heat the sample and to monitor its temperature when it was not being heated.

The magnetometer and solenoid were mounted inside a copper can filled with He gas. A superconducting magnetic shield made of 0.25-mm Pb foil completely enclosed the copper can and the assembly was immersed in a temperature-controlled helium bath. Glass Dewars were used and a two-layer Mu-metal shield enclosed the entire cryostat reducing the ambient magnetic field to about 1 mG.

Although the magnetometer could detect flux changes of $\sim 10^{-3}\ \Phi_0$, the absolute value of the flux change was known only to within $\pm\frac{1}{2}\%$. This absolute calibration was obtained from the known geometry of the calibration coil. It is necessary to take into account the difference in coupling of the calibration coil to the magnetometer ring and the sample to the ring. Also there is a small correction due to the diamagnetism of the sample in the small field produced by the feedback current. The calibration was checked by using the fact that when the feedback loop was opened, the output of the lock-in was a periodic function of the flux through the Nb ring with period Φ_0. The two procedures yield calibrations consistent within $\pm 1\%$.

Trapped-flux measurements were made using the following sequence: The sample cylinder was placed inside the upper solenoid in a known uniform magnetic field, cooled below the transition temperature T_c, then removed from the field and inserted into the magnetometer ring. It was then heated above its transition temperature and allowed to cool below T_c again. The change in magnetometer reading was a measure of the trapped flux. Some results are shown in Fig. 3. Several conclusions can be drawn from this data: For most values of the field the trapped flux is an integral multiple of Φ_0 within $\pm\frac{1}{2}\%$. The sizes of the steps are identical within $\frac{1}{2}\%$. The product of the incremental magnetic field between two steps and the cross-sectional area is Φ_0.

The measured values of trapped flux lying between integral multiples of Φ_0 are repeatable and independent of temperature from about 0.010 K below T_c to 2.0 K below. (Figure 4 indicates typical repeatability.) Further, the flux trapped at a given temperature is unchanged if the temperature is subsequently lowered, provided the wall thickness is much greater than λ for both temperatures.

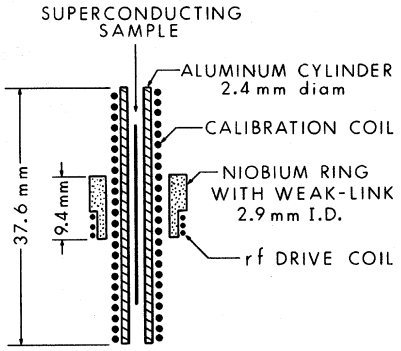

FIG. 2. Magnetometer configuration used for total flux measurements.

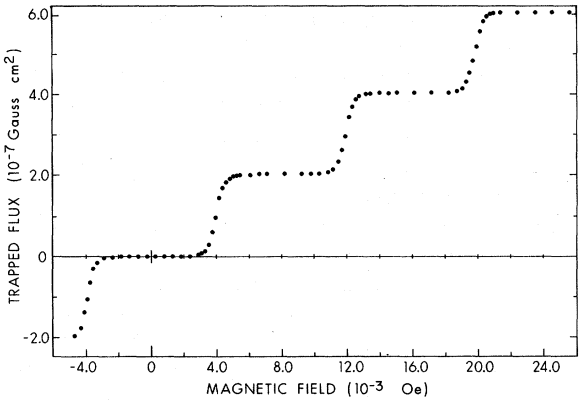

FIG. 3. Trapped flux as a function of the magnetic field in which the cylinder was cooled below its transition temperature. These data were taken with a tin cylinder, 56-μ i.d. and 24 mm long, with walls about 5000 Å thick.

Essentially identical results were obtained for cylinders with walls from 0.7–5 μ thick. A depression of the trapped flux by 3.5% from Φ_0 was observed for a cylinder with walls 0.14 μ thick. Since for this cylinder the assumption that the wall thickness is large compared to λ is not valid, the first integral in Eq. (1) is not negligible and a depression given by Eq. (3) would be expected. Considering the uncertainties in both the penetration depth and the film thickness the agreement is reasonable.

Initially the points lying between full quantized values in Fig. 3 were very puzzling. However, after more detailed measurements revealed the domain structure (which will be discussed in Sec. III) the interpretation of these points became clear. Since bands along the cylinder can exist in different quantized flux states, appropriate distributions of the bands along the length of the cylinder can permit the average flux in the cylinder to vary almost continuously. The large Nb ring magnetometer used for these measurements senses the net flux linking the Nb ring, so it measures essentially an average of the flux in the cylinder over a length approximately equal to the diameter of the ring.

By a second kind of measurement using this magnetometer we were able to determine that the particular distribution of bands was chosen when the cylinder was cooled through its transition temperature in the presence of the applied field and the distribution was not changed when the field was turned off. For these measurements a uniform field was applied within the Nb ring by means of the calibration coil. The sample cylinder was cooled through T_c in zero applied field outside the magnetometer and then inserted into the magnetometer ring. The resulting flux changes corresponded to the expulsion of the applied field from the total cross-sectional area of the sample and yielded the straight line in Fig. 5. (This provides still another means of calibrating the magnetometer and is consistent with the two previously mentioned ones though not as accurate since the area of the sample is not so precisely known.) The sample was then heated and allowed to cool again through the transition temperature in the applied field. The flux change then observed yields the lower curve in Fig. 5 and corresponds to the magnetization of the cylinder in the applied field. Finally, the applied field was turned off, the sample heated above the transition temperature, and the corresponding flux change measured, giving the trapped-flux curve shown in the upper part of Fig. 5. The difference between the straight line and the lower curve gives exactly the trapped flux curve, indicating as stated above that the particular mixed state is chosen when the cylinder is cooled through T_c in the field and is unchanged when the field is turned off.

III. DETAILED FLUX MEASUREMENTS

Prompted originally by the suggestion of Pierce that a domain-type structure might exist, we modified the large ring magnetometer by adding a pair of superconducting coils connected in a continuous circuit to transfer flux from a small sensing coil into the magnetometer. The small coil gave much better spatial resolution and permitted measurements of flux as a function of position along the cylinder. These measurements gave compelling evidence for the existence of just such a domain structure.[35]

Subsequently, we used another configuration of

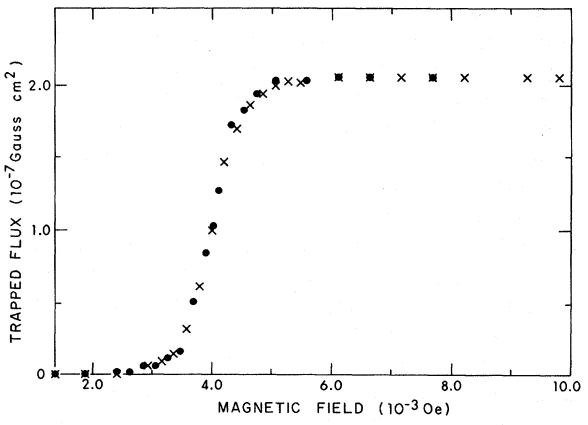

FIG. 4. Trapped flux as a function of the field in which the cylinder was cooled through its transition temperature. These data were taken with the same cylinder used for the data in Fig. 3. The dots and crosses are data from two different runs at 3.68 and 3.60 K, respectively.

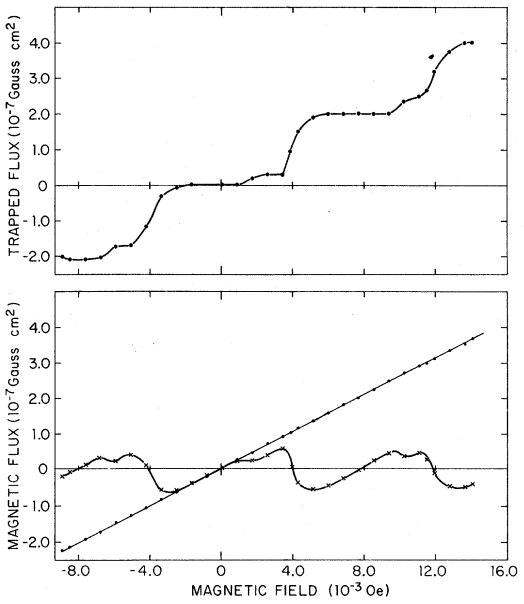

FIG. 5. Upper: Trapped flux as a function of the magnetic field in which the cylinder was cooled below the superconducting transition temperature. Lower: Flux produced by the cylinder in the field in which it was cooled below the transition temperature. The straight line shows the flux produced by the cylinder when it is inserted into the applied field already superconducting and with no flux trapped.

the magnetometer, shown in Fig. 6, for improved spatial resolution. This magnetometer is similar to one described by Zimmerman *et al.*[38] It was operated using the same circuits (Fig. 2) as for the Nb ring magnetometer and was mounted similarly. For these measurements the sample cylinders were not enclosed in glass tubes so that the pick-up loop could be as close as possible to the cylinder. As before, flux was trapped in the cylinder by cooling it through its transition temperature in an applied field, and then the field was turned off. The cylinder was then passed slowly through the small loop and the magnetometer output was recorded as a function of position.

Many cylinders (14-, 28-, or 56-μ i.d., with wall thickness 1000–5000 Å) were mapped in this way and all showed the same general behavior. A representative set of maps is shown in Fig. 7. These data were obtained with a cylinder approximately the same diameter (56 μ) as that used for the data in Fig. 3. The map at the bottom of the figure shows the output of the magnetometer when the cylinder is completely normal. The curve shows randomly distributed magnetic impurities in the normal cylinder and the pattern is completely reproducible when the mapping is repeated several times. (We estimate that 0.1–1 ppm of ferromagnetic impurity in the wire would account for this background.)

Each of the maps above this one is labeled with the value of the applied magnetic field in which the cylinder was cooled through the transition temperature.

The map for $H = 0.84$ mOe shows that almost the entire cylinder is in the zero quantum state. The trace is much smoother indicating that most of the magnetic impurities are inside the superconducting cylinder and are screened from the pick-up loop; the extent of the cylinder is clearly evident from 4–19 mm. The two sharp spikes probably result from two bands in the $n = 1$ quantum state that are too small to be completely resolved by the pick-up loop. The small offset of the curve in the negative direction indicates that the ambient field at the pick-up loop is not zero and is producing a small diamagnetic signal.

The sequence of maps for 2.52–4.62 mOe corresponds to total flux values lying on the curve between zero and the first step in Fig. 3. For this range of trapping fields there are some regions with trapped flux and others with none. Small field changes cause large changes in the flux pattern (cf. curves for 4.20 and 4.45 mOe). For fields less than approximately 4 mOe, bands exist either in the zero-flux state ($n = 0$) or with one flux unit trapped ($n = 1$), with most of the cylinder having $n = 0$. For fields slightly larger than 4 mOe, the pattern is inverted with most of the cylinder having one flux unit trapped.

The map labeled $H = 2.52$ mOe already indicates a large band in the $n = 1$ quantum state near the left end of the cylinder along with some smaller bands. As the applied field is increased, more of the cylinder is in the $n = 1$ state until, in the map for $H = 6.30$ mOe, all of the cylinder is in the $n = 1$ state except for two small bands corresponding to two of the large magnetic impurities in the bottom maps of the normal cylinder. The top curve is a map with all of the cylinder in the $n = 2$ state ex-

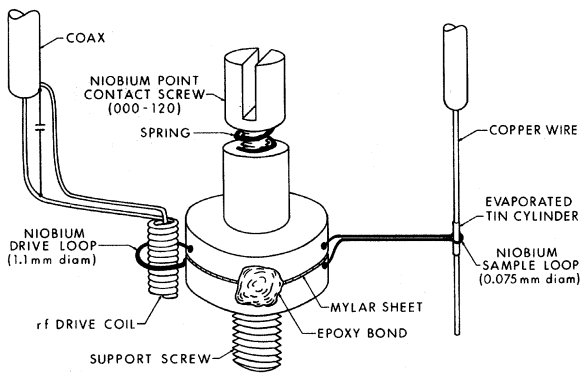

FIG. 6. Magnetometer configuration used for measuring flux as a function of position along the cylinder.

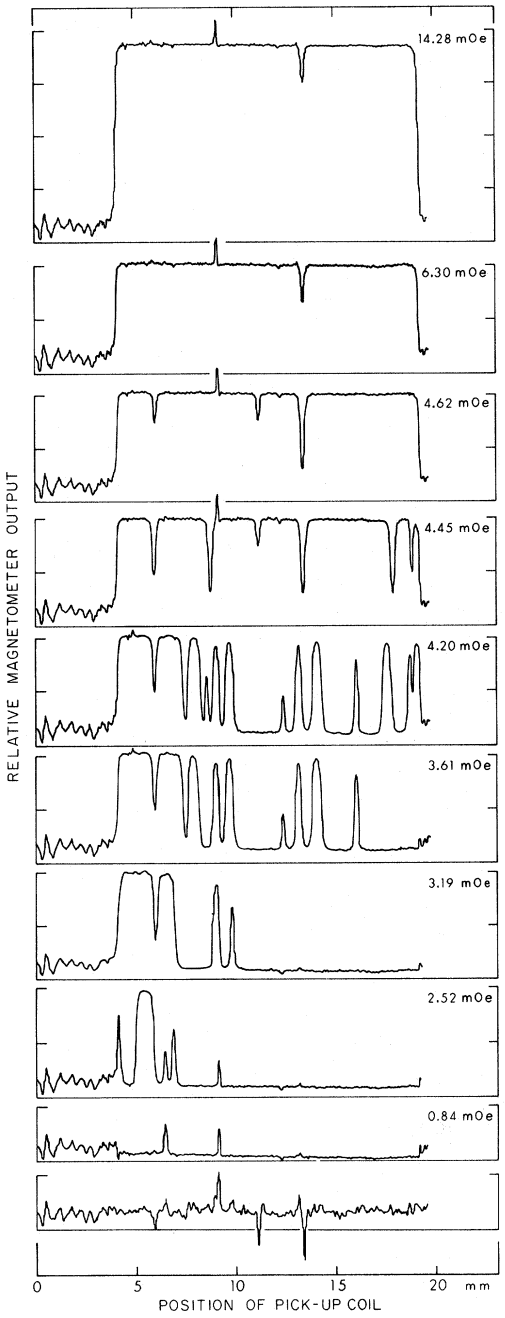

FIG. 7. Magnetometer output as a function of position of the pickup coil along the length of the cylinder. The curves are labeled with the values of applied field in which the cylinder was cooled through its transition temperature.

cept for the same two small bands. We have made sequences of maps up through 12 flux units trapped and find that this pattern repeats regularly. In general, we find that for trapping fields corresponding to points between the n and $n+1$ steps in Fig. 3, the flux maps indicate regions with no less than n flux units and no more than $n+1$ flux units.

By integrating the curve of flux versus position, the average flux trapped in the cylinder can be determined. We have done this for a sequence of 41 maps corresponding to applied fields from 0 to 25 mOe and to trapped flux values from 0 to $3\Phi_0$. The results are shown in Fig. 8 and they agree very well with the trapped flux curve determined with the large Nb ring magnetometer (Fig. 3).

It is possible to have the cylinder exhibit more complicated flux patterns by trapping flux, slowly warming the cylinder, then quickly recooling as the flux begins to change. In one map following this procedure we found bands corresponding to $n=1$, 2, and 3.

For a perfectly uniform cylinder in a completely uniform field along its axis, we might expect that the bands would be randomly distributed, being determined by fluctuations as the cylinder is cooled through T_c. The fact that the flux is trapped repeatably in the same patterns in our cylinders indicates that nucleation in a particular state is determined largely by the nonuniformities, particularly the magnetic impurities, in the substrate.

IV. TEMPERATURE DEPENDENCE OF TRAPPED FLUX

With the same magnetometer configuration used for mapping the flux distribution, we were able to measure the trapped flux as a function of temperature. The cylinder was cooled well below its transition temperature in an applied field which produced a flux distribution like that for $H=6.30$ mOe in Fig. 7, with essentially the entire cylinder in the $n=1$ quantum state. Then the loop was positioned well away from the end of the cylinder and from the intense magnetic impurities, and the magnetometer reading was plotted as the temperature was increased.

As the temperature approached T_c there was in

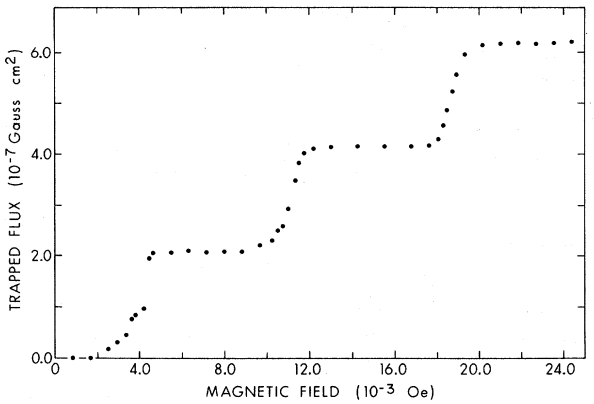

FIG. 8. Average flux in the cylinder as a function of applied field. Each point corresponds to the area under a corresponding flux distribution curve (Fig. 7).

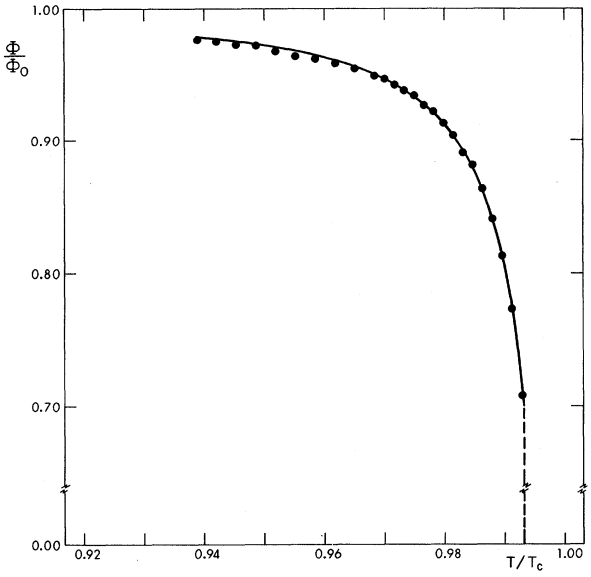

FIG. 9. Trapped flux as a function of temperature. The points are data for a tin cylinder (14-μ i.d., 5000-Å walls, 1 cm long), in a state with $n=1$. The curve is a fit to Eq. (4). The dashed line indicates a jump to the zero flux state.

general a continuous decrease in flux followed by an abrupt jump. Often the jump was to zero flux; in these cases remapping the distribution showed that a part of the cylinder 0.1–1 mm long, directly beneath the original position of the loop, had changed to the $n=0$ state. Sometimes there were smaller abrupt jumps; in these cases remapping showed that a band within a few hundredths of a millimeter of the original loop position had changed to the $n=0$ state. Usually it was possible to observe the trapped flux decrease by ~ 20% before a jump occurred. For one cylinder a continuous decrease of about 30% was observed. The measured flux as a function of reduced temperature for this cylinder is shown in Fig. 9, where the points indicate values read off the continuous flux plot.

For any point before the abrupt jump, lowering the temperature again restored the full original flux value and remapping indicated the same uniform distribution of flux.

There have been several calculations[16,18,19,24,25] of the magnetic flux in a long superconducting cylinder. When $r \gg \lambda$,

$$\varphi = \Phi_0 \left(1 - \frac{2\lambda_0}{r} \frac{x}{\sinh \alpha/x}\right) , \tag{4}$$

with

$$x = [1 - (T/T_c)^4]^{-1/2} \text{ and } \alpha = w/\lambda_0 ,$$

where λ_0 is the value of the penetration depth at $T=0$, r is the inner radius of the cylinder, w is the wall thickness, and T_c is the transition temperature. This result is equivalent to Eq. (3) for $T/T_c \approx 1$.

The curve plotted in Fig. 9 is a best fit of Eq. (4) to our data using T_c and α as parameters. A value of λ_0 is obtained from the slope of $\Delta\varphi$ versus $x/[\sinh(\alpha/x)]$. The values $T_c = 3.745$ K, $\alpha = 4.0$, and $\lambda_0 = 1200$ Å, obtained from this fit, are consistent with the measured $T_c = 3.75$ K, the estimated wall thickness of ~5000 Å, and the penetration depth found in similarly prepared Sn films.

V. SUMMARY AND DISCUSSION OF RESULTS

The results of our experiments can be summarized by several general statements about the quantized flux states of these superconducting cylinders. For most values of the applied magnetic field the trapped flux is distributed uniformly throughout the entire cylinder and is $n\Phi_0 \pm \frac{1}{2}\%$. For some values of the applied field a mixed state occurs with bands along the cylinder in states differing by one flux quantum. These bands are distributed in such a way that the average flux in the cylinder appears to vary almost continuously as a function of applied field. The particular distribution of bands is determined as the cylinder cools through the transition temperature in the presence of the applied field and is not significantly altered when the field is turned off. The distribution is independent of temperature from about 0.01 K to several kelvins below T_c.

When the cylinder is in a uniform state with one flux quantum in the entire cylinder, the trapped flux is found to vary reversibly with temperature in just the way required to maintain the constancy of the fluxoid.

Pierce first suggested that superconducting cylinders might exhibit a reasonably regular domain structure with small grain size (for example, bands of length comparable to the diameter of the cylinder). He hypothesized that superconductivity nucleates in a number of regions along the cylinder as it is cooled through the transition temperature, and that these regions may nucleate in different quantum states. They subsequently grow to fill the cylinder and, where two regions of different n meet, a vortex is formed. He used the Landau-Ginsburg theory to show that even for temperatures very near T_c, the vortices are very strongly pinned for even slight inhomogeneities in the cylinder wall; thus the domain structure is stable against changes in field and temperature. He also considered the problem of nucleation in different states and showed that ultimately thermodynamic fluctuations should produce a random distribution of domains along the cylinder.

Since the spatial distribution of the domains in our cylinders is very reproducible, it is most likely that the large biases produced by the magnetic impurities in the copper wire determine the domain pattern. Also, slight inhomogeneity in the field and nonuniformity of the cylinder tend to cause nucleation in the quantum state of larger n preferentially at one end of the cylinder.

The distribution of bands of alternating quantum number separated by pinned vortices can be pictured as a quantized flux line weaving in and out of the wall of the cylinder. The possibility of a flux line leaking through the wall at a normal spot was cited as a possible explanation for measured values of flux lying between quantized states in the original measurements.[3-5] Our experiments show that it was very likely that a domain structure existed in cylinders used for those experiments and accounts for the intermediate values since the average flux or total magnetization was being sensed.

Individual quanta trapped in the walls of superconducting cylinders have been observed in other experiments. Lischke has used an electron interferometer to exhibit the escape of flux in single quanta along the length of cylinders of about 1-μ diam. He has observed a quantized band only 8 μ long. Some time ago Zimmerman and Mercereau[39] used a method very similar to the one used for our experiments to observe flux pinned as localized single quanta in solid Nb wires.

Although we always observed a domain structure in our cylinders, it seems possible that for sufficiently small thin-walled hollow cylinders the current density required to trap one flux quantum might be so large, and the pinning so small, that the structure would be unstable. Lischke has, in fact, observed flux creep in his small cylinders; however, there is a small heating of the cylinder by the electron beam in his experiments.

Our results for the variation of the trapped flux with temperature are in good agreement with theory and correspond to the adiabatic variation of a quantum state with $n = 1$. A possible explanation for the disagreement between our results and Lischke's results which show no temperature dependence could be the rearrangement of the domain structure as the temperature is raised. At a given cross section of the cylinder the flux may retain almost its full low-temperature value while the distribution of domains is changing at other sections of the cylinder. It may be that the net reversible change was too small to be observed before an irreversible shift of quantum state of the particular band being observed occurred. Another alternative, of course, is that although we expect both experiments to respond to $\vec{A}\cdot d\vec{s}$ along the path enclosing the cylinder (defined by the electron beam in one case or the pick-up loop in the other), this may not be true.

---

*Research supported by the National Science Foundation. Helium provided by the Office of Naval Research.

[1]F. London, Phys. Rev. 74, 562 (1948).
[2]F. London, *Superfluids* (Wiley, New York, 1950), Vol. I, p. 152.
[3]B. S. Deaver, Jr. and W. M. Fairbank, Phys. Rev. Letters 7, 43 (1961).
[4]R. Doll and M. Näbauer, Phys. Rev. Letters 7, 51 (1961).
[5]R. Doll and M. Näbauer, Z. Physik 169, 526 (1962).
[6]N. Byers and C. N. Yang, Phys. Rev. Letters 7, 46 (1961).
[7]L. Onsager, Phys. Rev. Letters 7, 50 (1961).
[8]J. M. Blatt, Phys. Rev. Letters 7, 82 (1961).
[9]J. Bardeen, Phys. Rev. Letters 7, 162 (1961).
[10]J. B. Keller and B. Zumino, Phys. Rev. Letters 7, 164 (1961).
[11]W. Brenig, Phys. Rev. Letters 7, 337 (1961).
[12]K. Maki and T. Tsuneto, Progr. Theoret. Phys. (Kyoto) 27, 228 (1962).
[13]A. Bohr and B. R. Mottelson, Phys. Rev. 125, 495 (1962).
[14]G. Lüders, Z. Naturforsch. 17a, 181 (1962).
[15]W. Weller, Z. Naturforsch. 17a, 182 (1962).
[16]H. J. Lipkin, M. Peshkin, and L. J. Tassie, Phys. Rev. 126, 116 (1962).
[17]W. Weller, Phys. Letters 1, 222 (1962).
[18]F. Schwabl and W. Thirring, Nuovo Cimento 25, 175 (1962).
[19]V. L. Ginsburg, Zh. Eksperim. i Teor. Fiz. 42, 299 (1962) [Sov. Phys. JETP 15, 207 (1962)].
[20]M. Peshkin and W. Tobocman, Phys. Rev. 127, 1865 (1962).
[21]F. Bloch and H. E. Rorschach, Phys. Rev. 128, 1697 (1962).
[22]M. Tinkham, Phys. Rev. 129, 2413 (1963).
[23]M. Peshkin, Phys. Rev. 132, 14 (1963).
[24]D. H. Douglass, Phys. Rev. 132, 513 (1963).
[25]L. P. Rapoport, Zh. Eksperim. i Teor. Fiz. 45, 1453 (1963) [Sov. Phys. JETP 18, 1003 (1964)].
[26]W. A. Little and R. D. Parks, Phys. Rev. Letters 9, 9 (1962).
[27]A. L. Kwiram and B. S. Deaver, Jr., Phys. Rev. Letters 13, 189 (1964).
[28]B. Lischke, Phys. Rev. Letters 22, 1366 (1969).
[29]B. Lischke, Z. Physik 237, 469 (1970).
[30]H. Boersch and B. Lischke, Z. Physik 237, 449 (1970).
[31]J. E. Mercereau and L. T. Crane, Phys. Letters 7, 25 (1963).
[32]J. E. Mercereau and L. T. Crane, Phys. Rev. Letters 12, 191 (1964).
[33]T. K. Hunt and J. E. Mercereau, Phys. Rev. 135, A944 (1964).
[34]B. Lischke, Z. Physik 239, 360 (1970).
[35]W. L. Goodman and B. S. Deaver, Jr., Phys. Rev. Letters 24, 870 (1970).
[36]J. M. Pierce, Phys. Rev. Letters 24, 874 (1970).
[37]A. H. Silver and J. E. Zimmerman, Phys. Rev. 157, 317 (1967).

[38]J. E. Zimmerman, P. Thiene, and J. T. Harding, J. Appl. Phys. 41, 1572 (1970).

[39]J. E. Zimmerman and J. E. Mercereau, Phys. Rev. Letters 13, 125 (1964).

PHYSICAL REVIEW B VOLUME 4, NUMBER 5 1 SEPTEMBER 1971

Magnetoacoustic Wave in an Electron-Hole Gas—Bismuth

C. Guthmann, J. P. D'Haenens, and A. Libchaber

Groupe de Physique des Solides, Ecole Normale Supérieure, 24 rue Lhomond, Paris 5°, France

(Received 19 October 1970)

This paper presents an experimental study in bismuth of the acoustic plasma wave at microwave frequencies. We have studied the coupling, in the presence of a dc magnetic field, of this wave to the Alfvén mode; experiments have been performed at two frequencies: 10 and 3 GHz. The 3-GHz transmission spectrometer devised by the authors shows very clearly the presence of the magnetoacoustic mode, while at 10 GHz hybrid and cyclotron resonances are mixed with the phenomenon studied. The electromagnetic theory of this phenomenon in the case of a collisionless isotropic plasma is recalled; the case of bismuth is then fully analyzed and compared with experiment. From the coupling of the two modes, $n\epsilon_0$ is obtained, where n is the carrier density and ϵ_0 the band overlap.

I. INTRODUCTION

Alfvén-wave propagation in bismuth has been extensively studied[1] since the original work of Buchsbaum and Galt.[2] Using compensated solid-state plasmas, McWhorter and May[3] have tried, unsuccessfully, to discover evidence for acoustic waves, in the electron-hole gas. Yokota[4] has studied the theoretical coupling of the compressional Alfvén mode with the magnetoacoustic wave in the presence of a magnetic field; this effect has been observed experimentally in bismuth by Lupatkin and Nanney[5] and, more recently, by D'Haenens and Libchaber.[6]

In this paper a theoretical and systematic experimental study of the magnetoacoustic mode in bismuth is presented.

In Sec. II, the electromagnetic theory of this phenomenon allows the analysis of the effect of temporal and spatial dispersion on the wave spectrum. In the same section, the dispersion equation of the compressional Alfvén wave and of the magnetoacoustic mode is obtained in the complex case of bismuth, from the knowledge of the conductivity tensor for an ellipsoidal Fermi surface in the spatial-dispersion regime (Appendix B). An important result is derived: The quantity $n\epsilon_0$ (where n is the carrier density and ϵ_0 the band overlap energy) can be obtained experimentally.

In Sec. III, the experimental apparatus used is presented, in particular, the two-strip-resonators transmission spectrometer used at 3 GHz.

In Sec. IV, the theoretical and experimental results are presented and compared at two frequencies: 9.65 and 2.80 GHz. It is shown that at 2.8 GHz the magnetoacoustic mode appears very clearly, while at 10 GHz hybrid and cyclotron resonance are mixed with the phenomenon studied.

In Appendix A, it is recalled that the magnetohydrodynamical model of the propagation and coupling of the compressional Alfvén wave with the acoustic wave can be applied to the collisionless plasma, when the direction of wave propagation is perpendicular to the magnetic field. This approach, a classical one for gaseous-plasma physicists does not yet seem to be widely known to solid-state physicists.

II. ELECTROMAGNETIC THEORY OF PROPAGATION OF COMPRESSIONAL ALFVÉN MODE AND ITS COUPLING WITH MAGNETOACOUSTIC MODE

In Sec. II A, we review the electromagnetic theory of the Alfvén and magnetoacoustic modes for an isotropic compensated plasma. In Sec. II B we study the limits of these results in the cyclotron-resonance ($\omega \sim \omega_c$) and nonlocal-dispersion ($qR \sim 1$) regime, where $\vec{q}$ is the wave vector and R the cyclotron radius. Finally, in Sec. II C we present the theory of these modes for an anisotropic plasma like bismuth.

A. Electromagnetic Theory of Coupling of the Compressional Alfvén Mode with the Magnetoacoustic Mode

The electromagnetic theory of the coupling of the compressional Alfvén mode with the magnetoacoustic mode has been described by Yokota.[4] Let us recall it briefly. Consider an isotropic degenerated compensated plasma gas with an electron (hole) Fermi energy ϵ_{Fe} (ϵ_{Fh}) and carrier density $n(n_e = n_h)$. The conductivity tensor, in a small spa-